Seismic analysis method of unreinforced masonry structures subjected to mainshockaftershock sequences

Zhang, Yongqun ; Wang, Zhuolin ; Jiang, Lixue ; Skalomenos, Konstantinos; Zhang, Dongbo

DOI:
10.1007/s10518-022-01334-x

License:
Other (please specify with Rights Statement)

Document Version
Peer reviewed version

Citation for published version (Harvard):
Zhang, Y, Wang, Z, Jiang, L, Skalomenos, K & Zhang, D 2022, 'Seismic analysis method of unreinforced masonry structures subjected to mainshockaftershock sequences', *Bulletin of Earthquake Engineering*, vol. 20, no. 5, pp. 2619-2641. https://doi.org/10.1007/s10518-022-01334-x

Seismic analysis method of unreinforced masonry structures subjected to mainshock-aftershock sequences

Yongqun Zhang[1], Zhuolin Wang[1], Lixue Jiang[1*], Konstantinos Skalomenos[2], and Dongbo Zhang[1]

Abstract

Aftershocks have the potential to further aggravate the damage of masonry structures caused by mainshock. To quantitatively analyze the effect of aftershocks, this paper investigates the seismic response of unreinforced masonry structures subjected to mainshock-aftershock (M-A) sequences. Firstly, an analytical method for estimating the maximum storey drift of masonry structures subjected to M-A sequences is proposed, which is based on the non-iterative equivalent linearization method and the soft-storey failure mechanism of multi-storey masonry structures. Then, a finite element method is employed to verify the effectiveness of the proposed method. Finally, a parametric analysis is performed to evaluate the effects of aftershock intensity, anti-seismic wall area ratio, site classes, number of storeys, and mortar strength on the seismic responses of masonry structures subjected to M-A sequences, respectively. The results indicate that an excellent agreement for the maximum storey drift (θ_{max}) between analytical and numerical results. The effect of aftershocks on masonry structures in plastic phase is more distinct than that in elastic phase. Furthermore, the effect of aftershocks on the θ_{max} of masonry structures can be ignored when the relative intensity of aftershock is less than 0.5, and the θ_{max} can increase by approximately 19.0% when the relative intensity of aftershock is equal to 1.0. Additionally, for the masonry structures subjected to M-A sequences, the effects of site classes on the θ_{max} cannot be ignored, the θ_{max} can decrease with increasing anti-seismic wall area ratio and mortar strength, and increases with increasing number of storeys.

Lixue Jiang
jkyjgs2020@163.com

1 Shanghai Key Laboratory of Engineering Structure Safety, Shanghai Research Institute of Building Sciences Co. Ltd, Shanghai, China.
2 Department of Civil Engineering, The University of Birmingham, B15 2TT, Edgbaston, Birmingham, United Kingdom.

Keywords Masonry structure, Equivalent linear system, Storey yield strength coefficient, Seismic analysis, Aftershock

1. Introduction

Earthquakes are not single events. It is common for a major earthquake (mainshock) to be followed by many earthquakes (aftershocks) with lower magnitude which usually originated at or near the rupture zone of the mainshock. Within 3 days after the Mw7.9 earthquake in Wenchuan on May 12, 2008, approximately 3 aftershocks with magnitudes greater than 6.0 occurred (Wang et al. 2020). For the Mw8.8 Chile earthquake on February 27, 2010, about 90 aftershocks with magnitudes larger than 5.0 were recorded (USGS 2010). In the Mw7.8 Nepal earthquake on April 25, 2015, 3 aftershocks with magnitudes larger than 6.0 were recorded within 15 days after the mainshock (Apil et al. 2015). Generally, there is no enough time to repair structures effectively due to the short interval between the mainshock and the aftershock (Yeo et al. 2009). Therefore, aftershocks have the potential to further increase damages significantly in the already damaged structures cuaused by the mainshock, resulting in aggravation of economic losses and casualties. For the Turkey Van earthquake sequences, 28,000 buildings were damaged in the Mw7.1 mainshock on October 23, 2011, while 35,000 buildings were damaged after the Mw5.6 aftershock on November 9, 2011 (Ates et al. 2013). For the New Zealand earthquake sequences, 100 people were injured in the Mw7.1 mainshock on September 4, 2010, but 185 people were killed in the Mw6.3 aftershock on February 22, 2011 (Gledhill et al. 2011). Thus, the effect of aftershock should be considered for the seismic performance assessment of building structures.

Several studies have focused on the effect of mainshock-aftershock (M-A) sequences on the seismic response of building structures. Among them, the nonlinear dynamic analysis method was usually employed to evaluate the structural behavior (e.g., displacement, storey drift, damage index) under artificial or recorded M-A sequences (Hatzigeorgiou and Liolios 2010; Goda and Salami 2014; Shen et al. 2019; Zhang et al. 2020; Shen et al. 2020; Wang et al. 2020). Noteworthily, the conclusions reached by different researchers diverged obviously. Li and Ellingwood (Li and Ellingwood 2010) found that aftershocks had a significant effect on structural damage, while Tesfamariam and Goda (2015) revealed that aftershocks had a relatively minor effect. The reason is that factors such as site conditions and aftershock intensity have a great influence on the results. To fully understand the effect of M-A sequences, incremental dynamic analysis (IDA) and Monte Carlo simulation have been applied to attain the structural vulnerability curve and study the effect of different aftershock intensities and earthquake regions (Raghunandan et al. 2015; Li et al. 2020).

The main focus in seismic assessment of masonry structures has been on mainshock analysis. Researchers carried out many quasi-static tests and shaking table tests to investigate the failure pattern, bearing capacity, deformation capacity, and energy dissipation capacity of masonry structures. A series of research results have provided a theoretical basis for the performance assessment of masonry structures subjected to single earthquakes (Tomaževič 2007; Mendes and Loureno 2014; Graziotti et al. 2017; Guerrini et al. 2017; Nakamura et al. 2017; Azizi-Bondarabadi et al. 2019; Tomić et al. 2021). Rinaldin and Amadio (2018) investigated the seismic behaviour of masonry structures under repeated earthquakes, a series of non-linear dynamic analyses were employed to estimate the cumulative damage occurred during the seismic sequence. The investigation has focused on the seismic response of masonry structures subjected to M-A sequences, including displacement and damage index. However, the peak ground acceleration (PGA) of the selected aftershocks in previous studies were equal or similar to that of mainshock, which was impractical to quantitatively analyze the effect of different aftershock intensities on the structural response. In addition, there is a lack of analysis on the effect of masonry structure characteristics, such as material strength, number of storeys and site conditions, to the structural response under M-A sequences.

This study aims to analyze the seismic response of masonry structures subjected to M-A sequences. Firstly, a seismic analysis method for determining the maximum storey drift of masonry structures is proposed based on the non-iterative equivalent linearization method and the soft-storey failure mechanism of multi-storey masonry structures. Then, the effectiveness of the proposed method is verified computationally using the finite element method on the basis of shaking table tests. Finally, the effects of aftershock intensity, anti-seismic wall area ratio, site classes, number of storeys, and mortar strength on the structural response are studied systematically.

2. Calculated method of masonry structures subjected to M-A sequences

2.1 Storey yield strength coefficient of masonry structures

The equivalent base shear method is adopted for calculating the horizontal seismic load in seismic analysis of masonry structures. It is assumed that the horizontal seismic load is distributed in an inverted triangle along with the height of the structure. For a masonry structure, the number of storeys is n, the building area of each storey is A_0, and the combined gravity load per unit building area is g_e. According to the *Code for seismic design of buildings* (GB50011–2010) (2010), the equivalent mass coefficient 0.85 is introduced to consider the high mode effects of multi-storey masonry structures as in EC 8(2004). G_{eq} is a combined gravity load, which is defined as 1.0 Dead load + 0.5 Live Load (GB50011–2010). α is the seismic influence coefficient of sequence-type earthquake, which indicates the intensity of M-A sequences. Since the natural period of vibration of masonry structures is generally between 0.1s and 0.5s, α is suggested to be equal to the maximum seismic influence coefficient $\alpha_{\max}$ (GB50011–2010). Thus, the total base shear force V_0 of the multi-storey masonry structure can be calculated as:

$$V_0 = \alpha \cdot G_{eq} = 0.85 \alpha g_e n A_0 \tag{1}$$

The seismic shear force V_i of i^{th} storey can be estimated as

$$V_i = 0.85 \alpha g_e A_0 \cdot \frac{(n+i)(n-i+1)}{(n+1)} \tag{2}$$

The plane and vertical layouts of the masonry structure of residential and office buildings are generally regular, and these multi-storey masonry structures mostly adopt reinforced concrete floors. The traditional method for calculating the vertical stress of the wall does not consider the joint operation of the transverse and longitudinal walls. Therefore, the vertical stresses of the transverse and longitudinal walls are quite different. Considering the fact that the transverse and longitudinal walls work together, the vertical stresses of the connected transverse and longitudinal walls tend to show a uniform distribution, and this trend is more obvious in the lower storeys (Zheng and Jiang 2014). For the convenience of analysis, it is assumed that the vertical stresses of the transverse and longitudinal walls in the same storey are equal, and the floor is assumed to be rigid, thus the average ultimate shear capacity of i^{th} storey can be estimated as

$$R_{ui} = A_{w,i} f_{vE,mi} = \rho_i A_0 f_{vE,mi} \tag{3}$$

where ρ_i is the anti-seismic wall area ratio in the calculation direction of the i^{th} storey, which can be expressed as the ratio of wall area $A_{w,i}$ in half-storey hight to A_0; ρ'_i is the anti-seismic wall area ratio in the orthogonal direction of the i^{th} storey.

The average seismic shear strength $f_{vE,mi}$ of the i^{th} storey is calculated as (GB50011–2010)

$$f_{vE,mi} = \zeta_{Ni} f_{v,mi} \tag{4}$$

$$f_{v,mi} = 0.125\sqrt{f_{2,i}} \tag{5}$$

$$\zeta_{Ni} = \frac{1}{1.20}\sqrt{1+\sigma_i / f_{v,mi}} \tag{6}$$

where, $f_{v,mi}$ is the average bond-slip strength of the masonry of the i^{th} storey; $f_{2,i}$ is the compressive strength of mortar of the i^{th} storey; ζ_{Ni} is the influence coefficient of vertical pressure of the i^{th} storey; σ_i is the average vertical compressive stress in the i^{th} storey due to gravity load, which be expressed as

$$\sigma_i = \frac{g_e(n-i+1)}{\rho_i + \rho'_i} \tag{7}$$

where ρ'_i is the anti-seismic wall area ratio in the orthogonal direction of the i^{th} storey.

Substitute Eq. (7) into Eq. (6), then ζ_{Ni} can be estimated by Eq. (8).

$$\varsigma_{Ni} = \frac{1}{1.20}\sqrt{1+\frac{8.33 g_e(n-i+1)}{(\rho_i+\rho'_i)\sqrt{f_{2,i}}}} \tag{8}$$

According to the Elastic-Perfectly-Plastic (EPP) model established by Tomazevic (2007) and Magenes et al. (1997), the yield strength is 0.9 times of the average ultimate capacity, so the storey yield strength coefficient of the i^{th} storey can be estimated as

$$\xi_i = \frac{0.9R_{ui}}{V_i} = \frac{0.9A_{w,i} f_{vE,mi}}{V_i} \tag{9}$$

Substitute Eq. (2) ~ Eq. (5) and Eq. (8) into Eq. (9), and the storey yield strength coefficient can be further obtained by

$$\xi_i = \frac{0.11\rho_i}{\alpha g_e} \cdot \frac{n+1}{(n+i)(n-i+1)}\sqrt{f_{2,i} + \frac{8.33 g_e(n-i+1)\sqrt{f_{2,i}}}{\rho_i + \rho'_i}} \tag{10}$$

For the bottom storey, Eq. (10) is simplified as

$$\xi_1 = \frac{0.11\rho_1}{\alpha g_e n}\sqrt{f_{2,1} + \frac{8.33 n g_e \sqrt{f_{2,1}}}{\rho_1 + \rho'_1}} \tag{11}$$

For single-storey masonry structures, the coefficient of 0.11 in Eq. (10) and Eq. (11) should be changed to 0.11×0.85=0.094.

For masonry structures, the strength reduction factor is calculated as

$$R = 1/\xi_{i,\min} \tag{12}$$

where $\xi_{i,\min}$ is the minimum yield strength coefficient of each storey.

If the bottom storey is the soft-storey, the strength reduction factor can be estimated as

$$R = \frac{1}{\xi_1} = \frac{\alpha n g_e}{0.11\rho_1\sqrt{f_2 + \frac{8.33 n g_e \sqrt{f_2}}{\rho_1 + \rho'_1}}} \tag{13}$$

where f_2 is the compressive strength of mortar of the bottom storey.

2.2 The yield displacement demand of the equivalent single-degree-of-freedom

Based on the roof displacement method for calculating the natural period of the structure and the displacement calculation method for the multi-limb wall and wall frame, and considering the influence of the bending deformation, shear deformation and coupling of the wall limbs, Jiang et al. (2018) proposed the calculation formula for the natural period $T_{0,e}$ of masonry structures, which can be calculated as

$$T_{0,e} = \left(0.132+0.050\frac{H}{B}\right)\sqrt{\frac{g_e}{f_m^{1.5} h\rho}} \cdot H \tag{14}$$

Where, H and B are the total height and width of masonry structure, respectively; h is the soft-storey height; f_m is the compressive strength of masonry.

The elastic spectral displacement S_{de} of the equivalent single-degree-of-freedom (SDOF) system is computed as (Fajfar 1999).

$$S_{de} = \frac{T_{0,e}^2}{4\pi^2} \cdot \alpha g \tag{15}$$

The yield spectral displacement S_{dy} of the SDOF system is computed as (Fajfar 1999).

$$S_{dy} = \frac{S_{de}}{R} = \frac{T_{0,e}^2}{4\pi^2} \cdot \frac{\alpha g}{R} \tag{16}$$

Eq. (13) is substituted into Eq. (16) to obtain the yield spectral displacement demand S_{dy} (Eq. (17)).

$$S_{dy} = 0.027 \cdot T_{0,e}^2 \cdot \frac{\rho_1}{n g_e}\sqrt{f_2 + \frac{8.33 n g_e \sqrt{f_2}}{\rho_1 + \rho'_1}} \tag{17}$$

2.3 The inelastic displacement demand of the equivalent SDOF

The equivalent linearization method can be used to estimate the inelastic displacement demand of existing structures subjected to earthquakes. It was adopted in the capacity spectrum method of ATC-40. In this method, the displacement demand of a structure can be determined by the displacement demand of an equivalent linear system with an equivalent period and equivalent damping. The evaluation targets including equivalent period and equivalent damping are functions of the ductility coefficient, so an iterative process is employed to determine the displacement demand of existing structures. Meanwhile, an underestimate of displacement demand of existing structures may result from the equivalent damping which is independent of the natural period in the capacity spectrum method of ATC-40. To solve the above problems, an equivalent linear system based on the secant period was proposed by Lin and Lin (2009). In this method, the equivalent period and equivalent damping of the equivalent linear system are functions of the strength reduction factor. Since the strength reduction factor is known, iteration in determining the response of structures can be avoided effectively.

When the secant stiffness of the maximum displacement point is taken as the equivalent stiffness of the elastic-plastic model, the equivalent elastic period T_{eq} is calculated as (Borzi et al. 2001)

$$T_{eq} = T_{0,e}\sqrt{\frac{\mu}{1+\alpha_s\left(\mu-1\right)}} \tag{18}$$

where α_s is the post-yield stiffness; μ is the ductility factor which is the ratio of the maximum displacement to the yield displacement.

Base on the R-μ-T relationship, the μ in Eq. (18) can be replaced by the strength reduction factor R. According to the R-μ-T relationship proposed by Newmark and Hall (1973), $\mu=(R^2+1)/2$ can be substituted into Eq. (18) in short period region, while $\mu=R$ can be substituted into Eq. (18) in long period region. For M-A sequences, Zhai et al. (2015) and Zhang et al. (2017; 2020) express the ductility factor μ with strength reduction factor R through the R-μ-T relationship, these expressions clearly indicate the influence of different aftershock intensity. In this manuscript, the strength reduction factor R is computed by Eq. (19).

$$R = 1 + \frac{a_0\left(a_1T_{0,e}+T_{0,e}^2\right)\left(a_4+\mu\right)}{\left(1+a_2T_{0,e}+a_3T_{0,e}^2\right)\left(1+a_5\mu\right)}\frac{1}{0.87+0.08e^{1.2\gamma}} \tag{19}$$

where γ is the relative intensity of aftershock defined as the ratio of the peak ground acceleration of the aftershock (PGA_{as}) to that of the mainshock (PGA_{ms}); a_0, a_1, a_2, a_3, a_4 and a_5 are regression parameters depending on the site classes as listed in Table 1. The site classes are classified according to V_{20} referring to *Code for seismic design of buildings* (GB50011–

2010), and the corresponding V_{30} ranges are also listed in Table 1. μ can be calculated according to the inverse function of Eq. (19).

Table 1. The value of a_0~a_5

Parameter	V_{20}	V_{30}	a_0	a_1	a_2	a_3	a_4	a_5
Site class I	V_{20} > 500m/s	V_{30} > 596m/s	0.86	10.83	9.68	0.57	-0.79	0.02
Site class II	250m/s < V_{20} ≤ 500m/s	278m/s < V_{30} ≤ 596m/s	0.71	13.21	9.97	0.98	-0.84	0.01
Site class III	150m/s < V_{20} ≤ 250m/s	158m/s < V_{30} ≤ 278m/s	1.03	10.93	11.49	0.77	-0.95	0.04
Site class IV	V_{20} ≤ 150m/s	V_{30} ≤158m/s	0.66	13.25	9.95	0.55	-0.81	0.01

Considering the effect of M-A sequences on elastic spectra, the maximum seismic influence coefficient $\alpha_{\max}$ of M-A sequences can be expressed as $\alpha_{\max}$=2.25·PGA$_{ms}$·(1+0.03·γ) (Zhang 2020).

The equivalent damping ζ_{eq} of the EPP model is calculated as (Lin and Lin 2009)

$$\zeta_{eq} = \zeta_0 + 0.079 T_{0,e}^{-0.252} \sqrt{R-1} \tag{20}$$

where ζ_0 is the inherent damping.

According to the *General rule for performance-based seismic design of buildings* (CECS 160: 2004) (2004), the damping reduction factor of the EPP model can be obtained by Eq. (21).

$$B = \begin{cases} 1 + \dfrac{0.05-\zeta_{eq}}{0.06+1.4\zeta_{eq}} & (T_{eq} \le T_g) \\ \left(1 + \dfrac{0.05-\zeta_{eq}}{0.06+1.4\zeta_{eq}}\right) \cdot \left(\dfrac{T_g}{T_{eq}}\right)^{0.9+\frac{0.05-\zeta_{eq}}{0.5+5\zeta_{eq}}} & (T_{eq} > T_g) \end{cases} \tag{21}$$

where T_g is the characteristic period of ground motion.

The inelastic spectral displacement S_{dp} of the SDOF system is calculated as (Fajfar 1999)

$$S_{dp} = \frac{T_{0,e}^2}{4\pi^2} \cdot \alpha g \cdot C = \frac{T_{eq}^2}{4\pi^2} \cdot \alpha g \cdot B \tag{22}$$

where, C is the inelastic displacement amplification factor, which can be estimated as

$$C = \left(\frac{T_{eq}}{T_{0,e}}\right)^2 \cdot B \tag{23}$$

The analysis shows that for the masonry structures built on site class III and site class IV, the condition of $T_{eq} \leq T_g$ is generally satisfied. Therefore, the inelastic displacement amplification factor C (Eq. (24)) is derived by substituting Eq. (18) and Eq. (21) into Eq. (23).

$$C = \frac{R^2+1}{2} \cdot \left(1 - \frac{0.079 T_{0,e}^{-0.252} \sqrt{R-1}}{0.13 + 0.1106 T_{0,e}^{-0.252} \sqrt{R-1}} \right) \tag{24}$$

2.4 The storey drift demand of masonry structures

Both earthquake damage investigations and shaking table tests have shown that the most common failure mode of masonry structures subjected to earthquakes is soft-storey failure mechanism caused by the shear failure of the walls between windows. The deformation mainly concentrates on a critical storey, which is generally the bottom storey, when the storey stiffness is relatively uniform (Wang 2008; Tomaževič and Weiss 2010). Therefore, the storey shear model is adopted to determine the deformation of masonry structures, while the soft-storey yielding mechanism is applied (Borzi et al. 2008).

Assuming that the vibration mode of masonry structures remains linear (inverted triangle) before yielding (Borzi et al. 2008), the yield displacement demand δ_y of the soft storey is calculated as

$$\delta_y = \frac{h}{\Gamma_h H} S_{dy} \tag{25}$$

where Γ_h is the modal height coefficient. Γ_h for a regular distributed mass is approximately 0.67.

For a vertically irregular masonry structure, it is assumed that its inelastic displacement is entirely generated by the soft storey. Thus, the inelastic displacement demand δ_p of the soft storey is calculated as (Priestley et al. 2007)

$$\delta_p = \delta_y + (S_{dp} - S_{dy}) \tag{26}$$

For a vertically regular masonry structure, assuming that the inelastic displacement is mostly generated by the soft storey with a small part generated by the adjacent storeys, the inelastic displacement demand δ_p of the soft storey is calculated as (Restrepo-Velez 2003)

$$\delta_p = \delta_y + \frac{S_{dp} - S_{dy}}{0.8 + 0.1n} \tag{27}$$

According to Eq. (26) and Eq. (27), the maximum storey drift $\theta_{\max}$ of masonry structures can be obtained by Eq. (28).

$$\theta_{\max} = \delta_p / h \tag{28}$$

The calculation flowchart of the $\theta_{\max}$ for unreinforced masonry structures subjected to M-A sequences is shown in Figure 1.

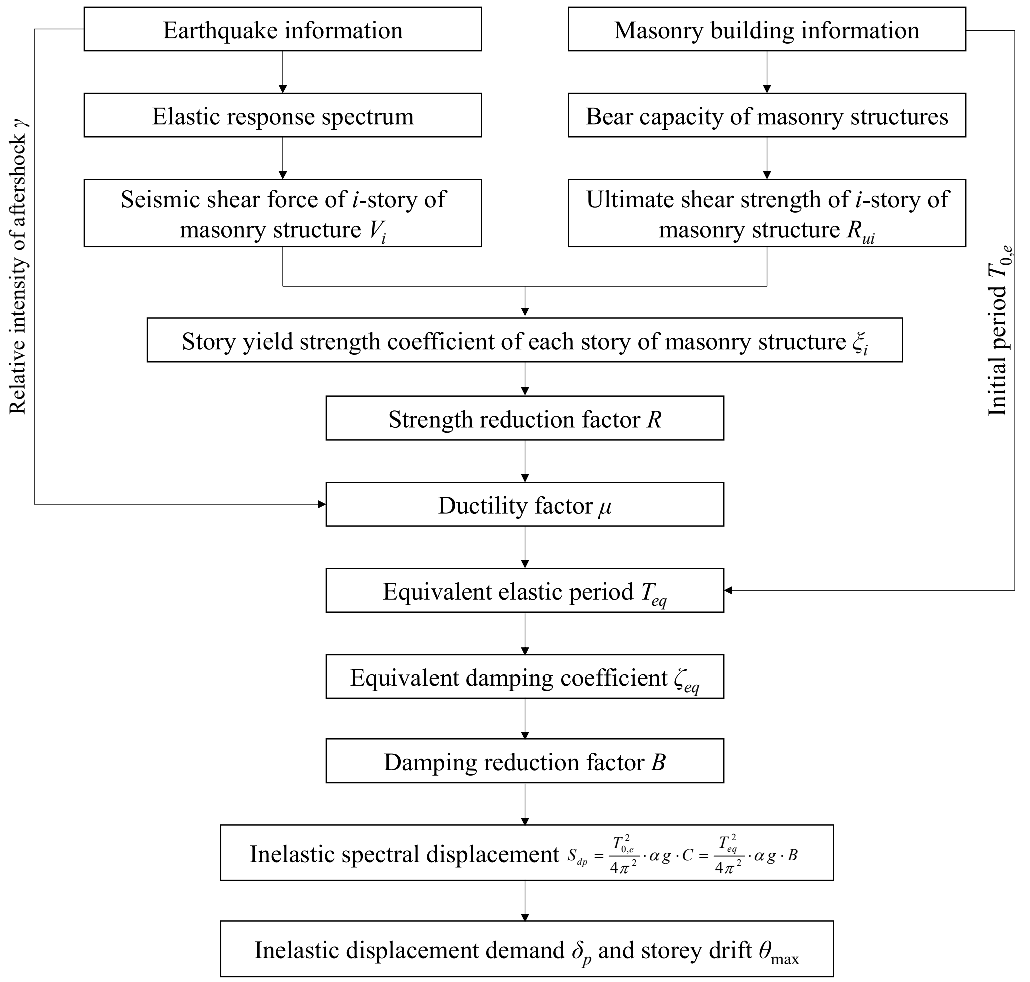

Figure 1. Calculation flowchart of the maximum storey drift $\theta_{\max}$ for masonry structures.

3. Validation of finite element model

The effectiveness of the method proposed in this manuscript is verified through a masonry residential building. The residential building model is a 5-storey masonry structure with a storey height of 3.0m, a width of 9.3m, and a length of 39.6m, as shown in Figure 2. The thicknesses of all masonry walls are 240mm, and the anti-seismic wall area ratio *ρ'* in the transverse direction and ρ in the longitudinal direction are 0.084 and 0.049 respectively. The combined gravity load per unit building area g_e is 1.0 Dead load + 0.5 Live Load = 11.0 kN/m^2, in which the dead load is the sum of the gravity load of the floor (4.0 kN/m^2) and the gravity load of the masonry walls (6.0 kN/m^2), and the live load is 2.0 kN/m^2. The compressive strength of brick clay and mixed mortar adopted in the current study are 10.0MPa and 2.0MPa, respectively. The compressive strength of masonry is 2.81MPa.

Initially, a part of the structure was modelled (the shaded part of the masonry structure shown in Figure 2). The correctness of the modeling method is verified by comparing the simulation results with the shaking table test results. Then, the whole structure is modelled (the whole masonry structure shown in Figure 2) to calculate the storey drift responses under M-A sequences. Finally, the results of the proposed method are compared with those obtained from the numerical simulations to verify the effectiveness of the proposed method.

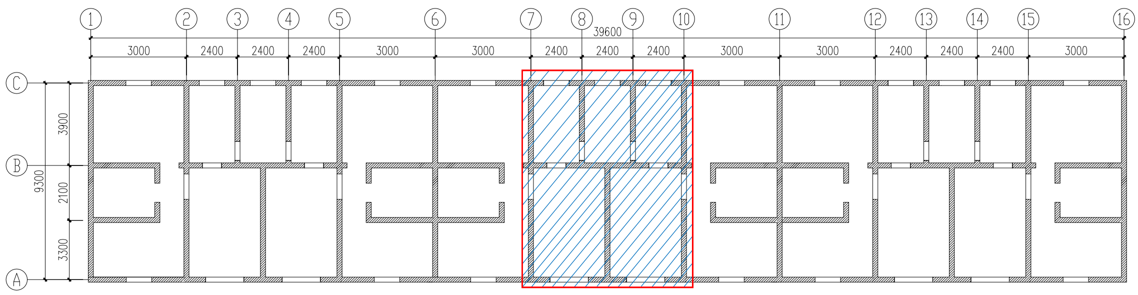

Figure 2. Plane of the unreinforced masonry structure model (unit: mm).

3.1 Validation of finite element model

The macro-modeling method simplifies the masonry into a homogenous material, and the mechanical properties of the homogenous material are determined by both the bricks and the mortar. The macro-modeling method ignores the difference of mechanical properties between bricks and mortar, as well as their interaction. Although the local behaviors of the masonry, such as crack localization and joint opening, are difficult to reproduce, satisfactory results can be obtained for the global responses and damage distribution with a low computational cost. Figure 3(a) illustrates the finite element model as a part of the whole structure as discussed in Figure 2. The model consists of masonry walls and reinforced concrete floor slabs. Multilayer shell elements with reduced integration were applied to simulate the nonlinear behavior of the masonry walls and the reinforced concrete floor. For the constitutive laws, the kinematic hardening model of the steel and the plasticity model of masonry and concrete with damage energy consumption were considered. The specific modeling method can be found elsewhere (Zhang and Wang 2013).

(a) (b)

Figure 3. Plan of the masonry structure (unit: mm): (a) Finite element model, (b) Experimental model.

To ensure the effectiveness of the subpart finite element model, the natural period of the masonry structure model is analyzed first. The seismic performance of a corresponding 1/4 scaled masonry structure was previously studied by shaking table tests. The results of this work can be found in Jiang et al. (2021) and the overview of the experiment is shown in Figure 3(b). The measured natural period of the scaled masonry structure model is 0.125s, and the similarity coefficient is 3.162:1, so the natural period of the prototype is 0.397s. The comparison between numerical and experimental results is shown in Table 2. The error between the numerical and experimental results is 0.76%, which is in good agreement.

Table 2. The comparison between numerical and experimental results.

Direction	Measured natural period/s	Analytical natural period/s	Numerical natural period /s	Analytical error/%	Numerical error/%
X-direction	0.397	0.395	0.394	-0.50	-0.76

El Centro wave and Taft wave were selected to study the displacement response of masonry structure. The comparison of roof displacement between the numerical results and the experimental results is shown in Figure 4. The roof displacement of the numerical results has taken the similarity coefficient 4:1 into consideration. The results show that the numerical curves are basically consistent with the experimental curves, the maximum top displacement of the numerical simulation is close to the maximum displacement of the experimental measurement, and the error is within 15%. Therefore, the numerical model can be used to study the seismic response of unreinforced masonry structures subjected to M-A sequences.

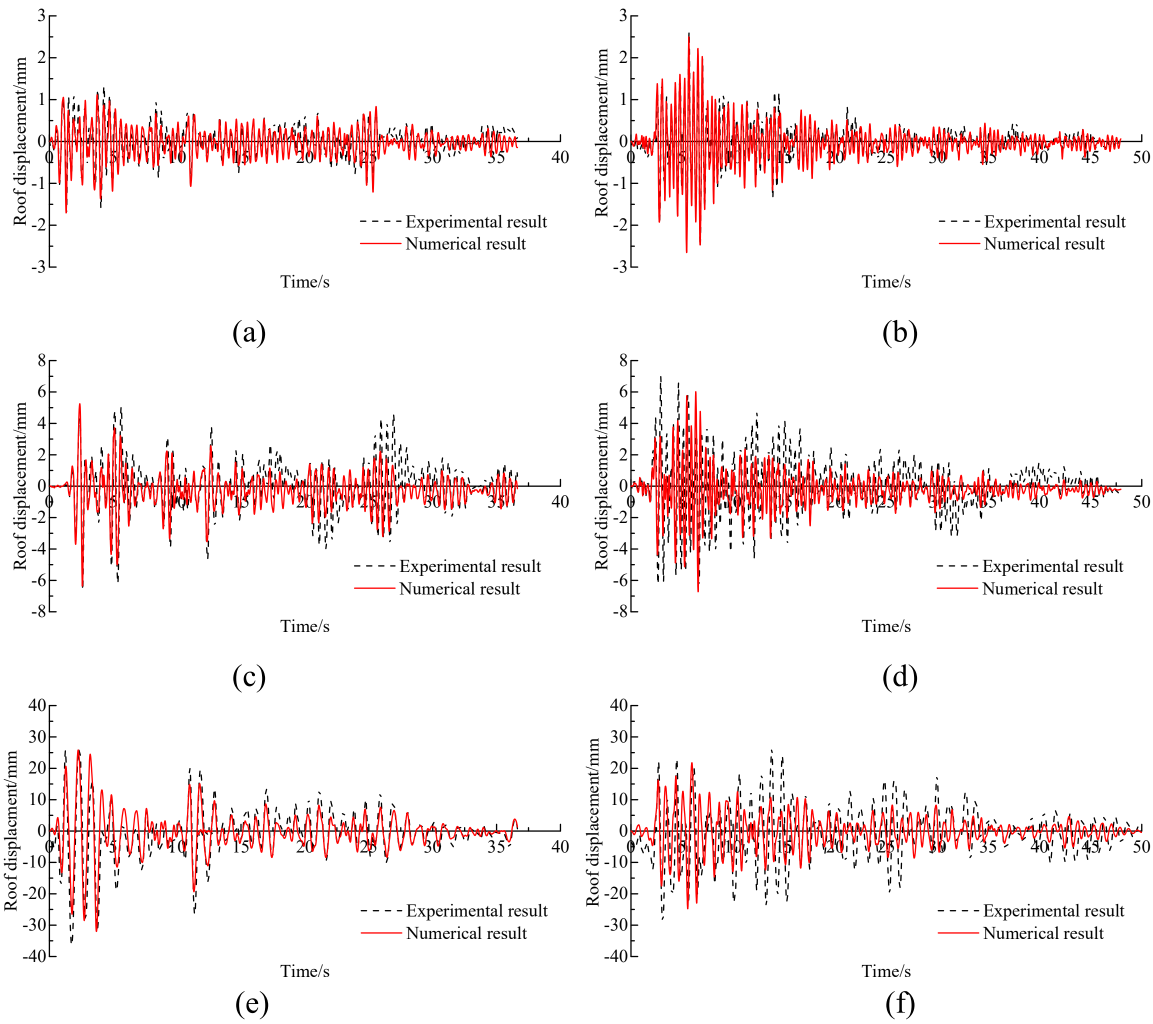

Figure 4. Comparison of roof displacements between numerical and experimental results: (a) El Centro, 0.035g, (b) Taft, 0.035g, (c) El Centro, 0.100g, (d) Taft, 0.100g, (e) El Centro, 0.200g, (f) Taft, 0.200g.

3.2 Comparison between finite element method and the proposed method

3.2.1 *Selected M-A sequences*

To accurately obtain the response of masonry structure subjected to M-A sequences, only real earthquake records are selected. Based on the selection principles proposed in previous research (Shen et al. 2019), 8 M-A sequence records for site class II are chosen from different earthquake events to consider earthquake uncertainty and listed in Table 3.

The magnitude of the mainshock in the actual M-A sequence is greater than that of the aftershock, so PGA_{ms} is generally not less than PGA_{as}. To study the impact of the relative intensity of aftershocks, γ is set to 0, 0.5, 0.8, and 1.0, respectively (γ=0 indicates mainshock only).

Table 3. Selected ground motion record of M-A sequence

Earthquake event	Seismograph station	M-A	Time	PGA	M_w
Managua,Nicaragua	Managua ESSO	Mainshock	1972/12/23 06:29	0.372	6.2
		Aftershock	1972/12/23 07:19	0.263	5.2
Mammoth Lakes	Long Valley Dam	Mainshock	1980/05/25 16:34	0.430	6.0
		Aftershock	1980/05/25 16:49	0.482	5.7
Kalamata, Greece	Kalamata	Mainshock	1986/09/13 17:25	0.235	6.2
		Aftershock	1986/09/15 11:41	0.241	5.4
Whittier Narrows	LA - Obregon Park	Mainshock	1987/10/01 14:42	0.428	6.0
		Aftershock	1987/10/04 10:59	0.344	5.3
Northridge	LA - Century City CC North	Mainshock	1994/01/17 12:31	0.256	6.7
		Aftershock	1994/01/17 12:32	0.162	6.1
Chichi	CHY029	Mainshock	1999/09/20 17:47	0.277	7.6
		Aftershock	1999/09/20 17:57	0.241	5.9
L'Aquila	GRAN SASSO	Mainshock	2009/04/06 01:33	0.145	6.3
		Aftershock	2009/04/07 17:47	0.252	5.6
East Japan Earthquake	CHB005	Mainshock	2011/03/11 13:46	0.180	9.0
		Aftershock	2011/03/11 15:15	0.175	7.7

3.2.2 *The effectiveness of the proposed method*

Using the validated modeling method introduced in Section 3.1, a finite element model of the whole structure is established based on the masonry structure shown in Figure 2 to verify the effectiveness of the proposed method. The comparison between analytical and experimental results is shown in Table 2. The error between the analytical and experimental results is 0.50%. The average storey drift of masonry structures under 8 M-A sequences was analyzed by the finite element method, and the storey drift of the masonry structure for site class II is also calculated by the proposed method. The comparison of the results is shown in Figure 5. For PGA_{ms} = 0.1g, the errors between the numerical results and the analytical results are within 11.0%. For PGA_{ms} = 0.2g, the errors between the numerical results and the analytical results are within 8.0%. It appears that the analytical results are in a good agreement with the numerical results.

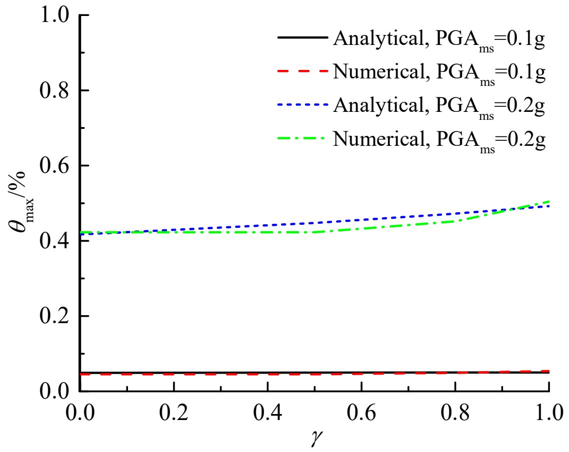

Figure 5. Comparison of analytical and numerical results.

4. Seismic analysis of unreinforced masonry structures subjected to M-A sequences

The 5-storey masonry structure shown in Figure 2 was used as a basic structure model to study the effect of M-A sequences on the seismic response of unreinforced masonry structures. The θ_{max} of the masonry structure for four site classes subjected to M-A sequences with γ = 0, 0.5, 0.8 and 1.0 are shown in Figure 6. As shown in Figure 6, the θ_{max} of the masonry structure shows the same trend of variation with increasing mainshock intensity regardless of the site class and the aftershock intensity.

For a given site class and PGA_{ms}, the θ_{max} of the masonry structure increases with increasing γ. For site class II and PGA_{ms}=0.2g, the θ_{max} of the masonry structure subjected M-A sequences with γ = 0, 0.5, 0.8 and 1.0 is 0.417%, 0.448%, 0.472%, and 0.491%, respectively, indicating that the aftershock can lead to a larger storey drift of masonry structures.

The performance level of a generic masonry structure is usually defined by roof displacement or storey drift. According to the research on the relationship between the performance level and the θ_{max} of masonry structures, three performance levels, namely *Light damage limit state* (LS1), *Significant damage limit state* (LS2), and *Collapse limit state* (LS3), are employed to describe the structural damage states. An average drift of 0.130%, 0.340%, and 0.720% can be used to identify the LS1, LS2, and LS3 limit conditions of unreinforced masonry structures (Borzi et al. 2008). For site class II, when the θ_{max} of the masonry structure reaches 0.720%, the PGA_{ms} of the M-A sequence with $\gamma = 0$, 0.5, 0.8, and 1.0 is 0.25g, 0.24g, 0.23g, and 0.23g, respectively, indicating that the larger the aftershock intensity is, the earlier the masonry structure reaches the limit state.

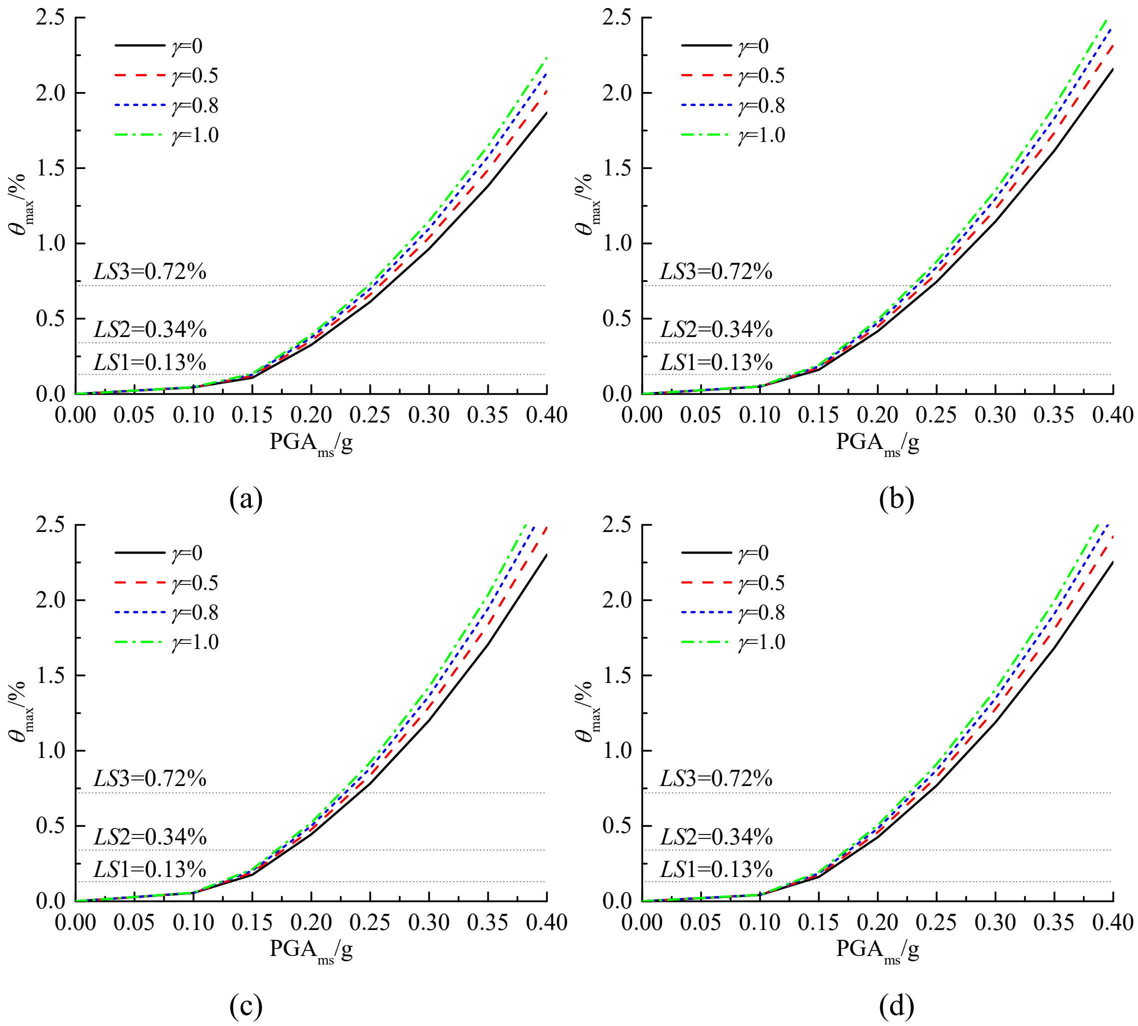

Figure 6. The θ_{max} of the 5-storey masonry structure for different site classes and M-A sequences with different γ: (a) site class I, (b) site class II, (c) site class III, (d) site class IV.

4.1 Effect of site class

To assess the effect of site classes on the seismic response of masonry structures, the θ_{max} of the reference structure model on different site classes is normalized by the mean θ_{max} of all site classes, respectively. In this way, the error of the θ_{max} without considering site conditions can be studied quantitatively. The normalized θ_{max} of the reference masonry structure model for the different site classes and M-A sequences (γ = 0.5, 0.8, and 1.0) is shown in Figure 7. Structures founded on site class I exhibit a lower θ_{max} value. This indicates that θ_{max} can be overestimated up to 19.2% for site class I if site class effect is ignored. Structures founded on site class II and site class III exhibit a higher θ_{max} value, indicating that site class effect can lead to underestimation of θ_{max} on site class II and site class III up to 4.8% and 17.6%, respectively.

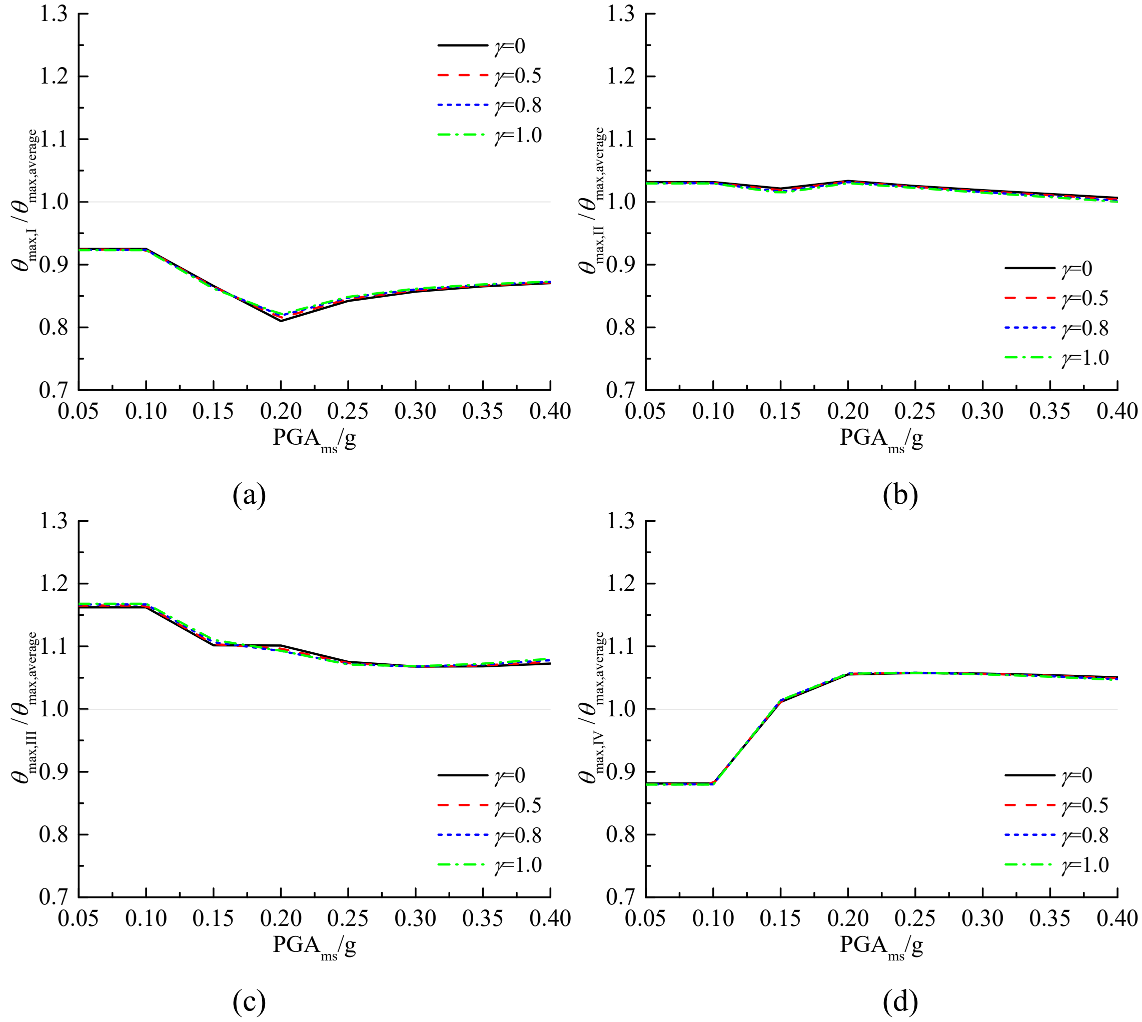

Figure 7. The $\theta_{max}/\theta_{max,average}$ of 5-storey masonry structure for different site class: (a) site class I, (b) site class II, (c) site class III, (d) site class IV.

4.2 Effect of the number of storeys

In order to investigate the effect of the number of storeys, n, on the seismic response of masonry structures, the n of the reference structure model is set to 1, 2, 3, 4, and 5 respectively, and other parameters of the reference structure model remain unchanged. The θ_{max} of the masonry structures subjected to M-A sequence with PGA_{ms}=0.2g are calculated, and the results are shown in Figure 8. According to GB50011-2010 (2010), when PGA_{ms} = 0.05g, 0.1g, and 0.2g, the θ_{max} of masonry structures should not exceed the limit of θ_{max} corresponding to LS1, LS2, and LS3, respectively. θ_{max} exceeding LS3 indicates the collapse of structures. Meanwhile, the variation law of θ_{max} for different PGA_{ms} is basically the same as the θ_{max} for PGA_{ms} = 0.2. Therefore, PGA_{ms} is taken as 0.2g for structural analysis in Section 4.2 and 4.3.

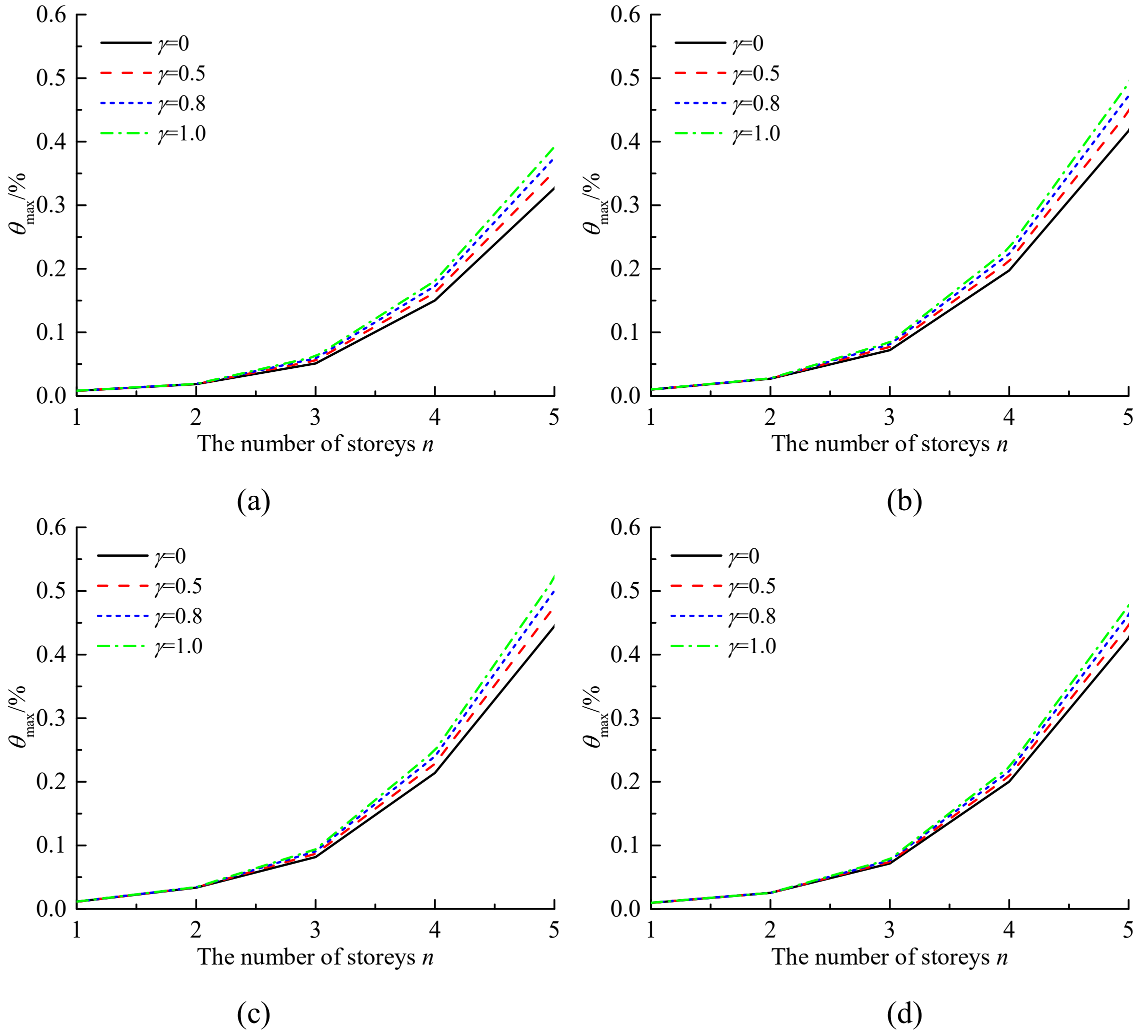

Figure 8. The θ_{max} of masonry structures for different number of storeys, PGA_{ms}=0.2g: (a) site class I, (b) site class II, (c) site class III, (d) site class IV.

Figure 8 shows that the θ_{max} of masonry structures with different n increase evidently with the increase of n. For PGA_{ms}=0.2g, γ=0, and site class II, the θ_{max} of masonry structures with n=1, 2, 3, 4, and 5 are 0.009%, 0.027%, 0.072%, 0.197%, and 0.417%, respectively. For PGA_{ms}=0.2g, γ=1.0 and site class II, the θ_{max} of masonry structures with n=1, 2, 3, 4, and 5 are

0.010%, 0.028%, 0.084%, 0.233%, and 0.491%, respectively. The results indicate that the *n* has a significant effect on the θ_{max} of masonry structures. The smaller the *n*, the greater the PGA_{ms} required for the masonry structure to enter the inelastic phase. The reason is that with the decrease of *n*, the anti-overturning requirements of the structure decrease, and the base shear force of the structure also decreases, that is, the plane layout and material strength of the 1-storey masonry structure and the 1st storey of the 5-storey masonry structure are completely consistent, both have the same seismic capacity, but the seismic shear load of the former is significantly less than that of the latter, resulting in the high-rise masonry structure entering the plastic phase with a smaller PGA_{ms}. It should be pointed out that the plane layout and material strength of the masonry structures with different *n* in this manuscript are consistent, so as to directly compare the effects of *n*. However, the anti-seismic wall area ratio ρ and the material strength of the actual low-rise masonry structure is generally smaller than that of the low-rise masonry structure in this manuscript, resulting in the seismic capacity of the former being smaller than that of the latter, that is, the low-rise masonry structure may damage in smaller PGA_{ms} in practice.

Earthquake damage investigations have showed that the damage degree of masonry structures is directly proportional to the *n* of masonry structures in the same intensity zone (Zhou 2011). The results of this manuscript are consistent with the earthquake damage investigation. Therefore, for high rise masonry structures, seismic strengthening (such as RC tie columns, ring beams etc.) and materials with higher strength must be adopted to meet the seismic requirements (Zhang et al. 2021).

To compare the effects of M-A sequences with different γ, the θ_{max} of masonry structures with γ = 0.5, 0.8 and 1.0 is normalized by the θ_{max} of the reference structure with γ = 0, as shown in Figure 9. Figure 9 indicates that the θ_{max} for M-A sequences was quite close to the θ_{max} for mainshock for a range of PGA_{ms} less than 0.31g, 0.20g, 0.16g, 0.13g, and 0.11g when *n*=1, 2, 3, 4, and 5, respectively. The reason is that the masonry structures behave elastically in the PGA_{ms} range, and the structural response mainly depends on the elastic spectra, but the difference of elastic spectra with different γ is small. Therefore, the effect of aftershocks can be ignored in elastic phase.

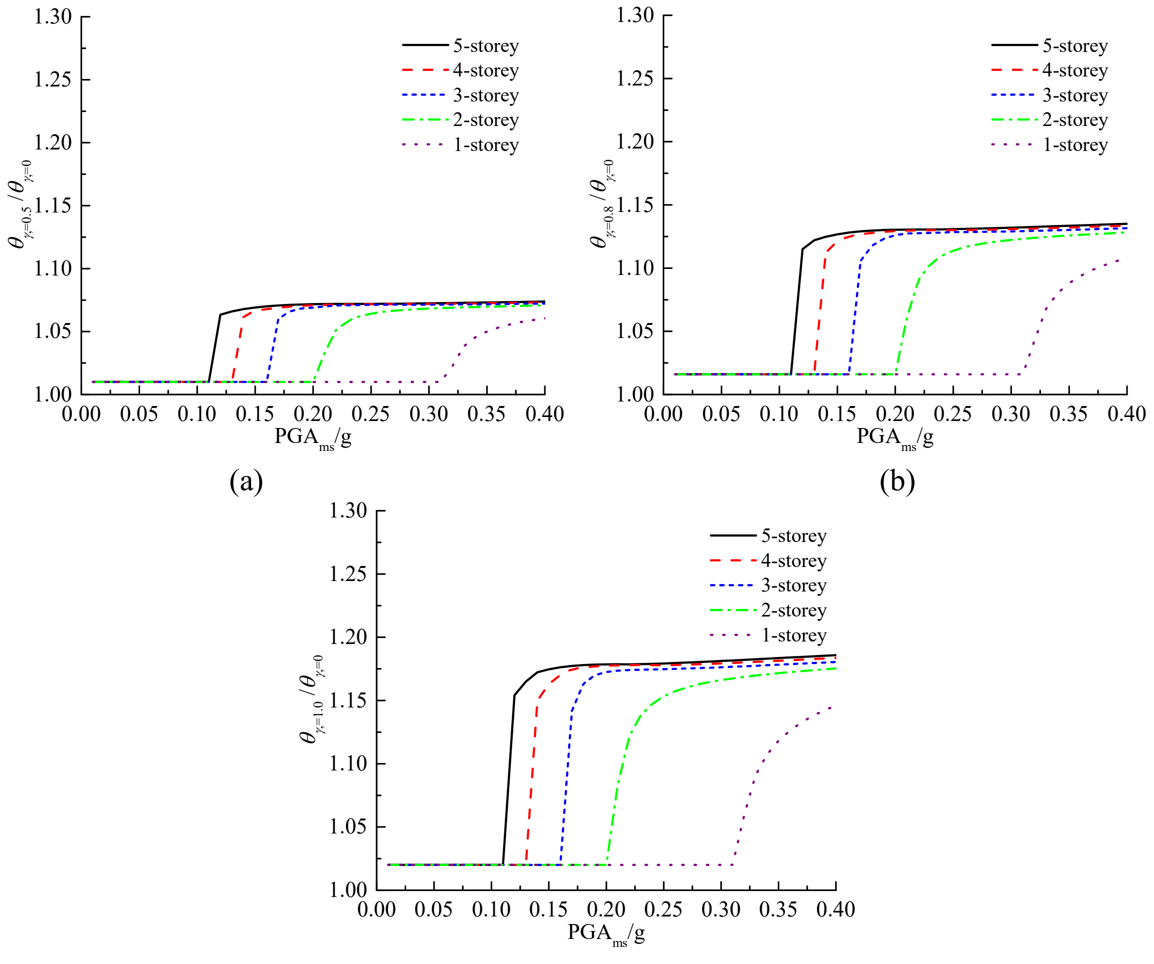

Figure 9. The $\theta_{\max,\gamma}/\theta_{\max,\gamma=0}$ of masonry structures for different γ and different n, site class II: (a) $\gamma = 0.5$, (b) $\gamma = 0.8$, (c) $\gamma = 1.0$.

The $\theta_{\max}$ for M-A sequences is significantly greater than that for only mainshock when PGA_{ms} is larger than 0.31g, 0.20g, 0.16g, 0.13g, and 0.11g for n=1, 2, 3, 4, and 5, respectively. The reason is that the masonry structures enter inelastic phase under the strong mainshock, and the damage degree of the structure is further aggravated due to aftershock energy. For γ=0.5, the $\theta_{\max}$ of masonry structure subjected to M-A sequences increases by 7.3%, indicating that the effect of aftershock with γ less than 0.5 can be negligible. For γ=0.8 and 1.0, the $\theta_{\max}$ of masonry structure subjected to M-A sequences increases by 13.1% and 19.0%, respectively. The result shows that the effect of aftershocks with γ more than 0.8 is significant and cannot be negligible.

The plane layout of masonry structures can be reflected by the anti-seismic wall area ratio ρ, which indicates the ratio of the total anti-seismic wall area at the 1/2-storey height to the storey area of the structure. To study the effect of ρ on the structural response, the ρ of the reference structure model is set to 0.021, 0.035, and 0.049, respectively. The θ_{max} of the masonry structures subjected to M-A sequence are calculated, and the results are shown in Figure 10.

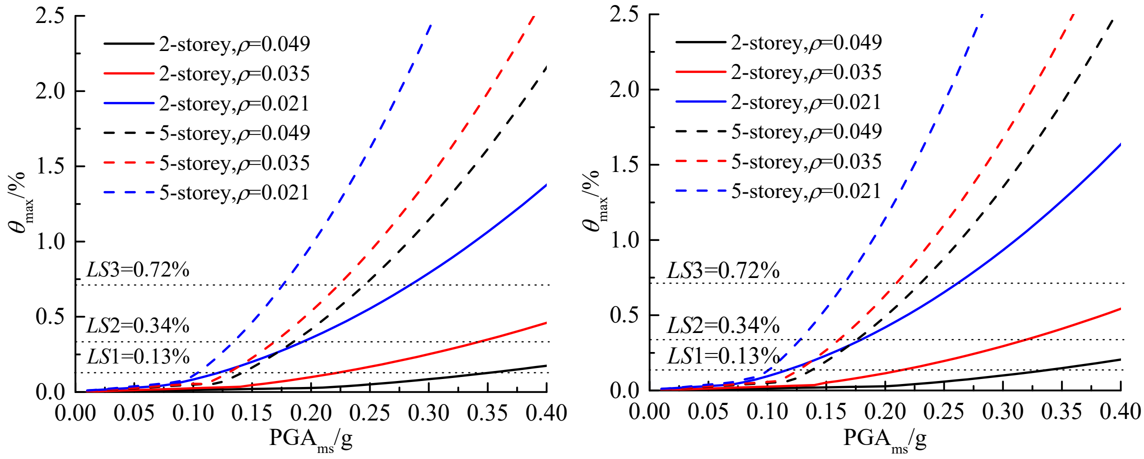

(a) (b)

Figure 10. The θ_{max} of masonry structures for different ρ and different n, site class II: (a) γ = 0, (b) γ = 1.0.

For PGA$_{ms}$=0.2g and γ = 0, the θ_{max} of the 5-storey masonry structures with ρ = 0.021, 0.035, and 0.049 are 0.971%, 0.536% and 0.417%, respectively. At the same seismic intensity, the θ_{max} of the 2-storey masonry structures with ρ = 0.021, 0.035, and 0.049 are 0.358%, 0.100% and 0.027%, respectively. For PGA$_{ms}$=0.2g and γ = 1.0, the θ_{max} of the 5-storey masonry structures with ρ = 0.021, 0.035, and 0.049 are 1.142%, 0.631% and 0.491%, respectively. At the same seismic intensity, the θ_{max} of the 2-storey masonry structures with ρ = 0.021, 0.035, and 0.049 are 0.419%, 0.115% and 0.028%, respectively. By decreasing the anti-seismic wall ratio from 0.049 to 0.035, the θ_{max} increases to 2.60 times on average, which shows that the θ_{max} of the masonry structures significantly increases with the decrease of ρ. The reason is that the seismic load is borne by the masonry walls along the earthquake load, and larger area of seismic wall will lead to greater shear capacity of the structure and smaller structural response. For 2-storey masonry structures in rural areas in China, the value of ρ is generally closer to 0.021. It can be seen from Figure 10 that the 2-storey masonry structure with ρ = 0.021 is seriously damaged when PGA$_{ms}$ = 0.2g, which is consistent with the earthquake damage investigation.

4.3 Effect of mortar strength

Mortar strength f_2 is an important factor affecting the shear capacity of masonry structures. To study the effect of f_2 on the θ_{max} of masonry structures subjected to M-A sequences, the f_2 of the reference structure model is set to 1.0MPa, 2.5 MPa, 5.0 MPa, 7.5 MPa, and 10.0 MPa, respectively, while other parameters of the reference structure model remain unchanged. The θ_{max} of the masonry structures with different mortar strengths for the four site classes subjected to M-A sequences with different γ are shown in Figure 11.

As shown in Figure 11, the θ_{max} of masonry structures decreases as the mortar strength increases. For PGA_{ms} = 0.2g, γ = 0, and site class II, the θ_{max} of 5-storey masonry structures with f_2= 1.0MPa, 2.5 MPa, 5.0 MPa, 7.5 MPa, and 10.0 MPa are 0.648%, 0.348%, 0.160%, 0.083%, and 0.044%, respectively. For PGA_{ms} = 0.2g, γ = 1.0, and site class II, the θ_{max} of 5-storey masonry structures with f_2= 1.0MPa, 2.5 MPa, 5.0 MPa, 7.5 MPa, and 10.0 MPa are 0.764%, 0.411%, 0.191%, 0.092%, and 0.046%, respectively. Overall, the θ_{max} of the masonry structure with f_2=2.5 MPa, 5.0 MPa, 7.5 MPa, and 10.0 MPa are 0.55, 0.25, 0.11, and 0.05 times of those with f_2=1.0 MPa, respectively, indicating that the mortar strength has a great influence on the structural response of masonry structures. The reason is that with the increase of mortar strength, the shear capacity of masonry increases, resulting in less structural damage. Therefore, the higher the mortar strength, the smaller the θ_{max}, and the better the seismic performance of the structures.

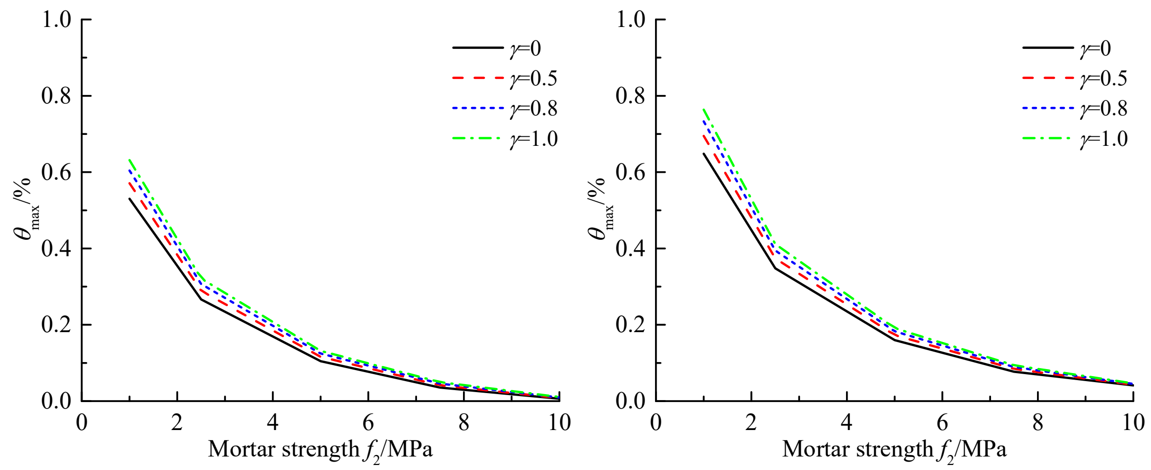

(a) (b)

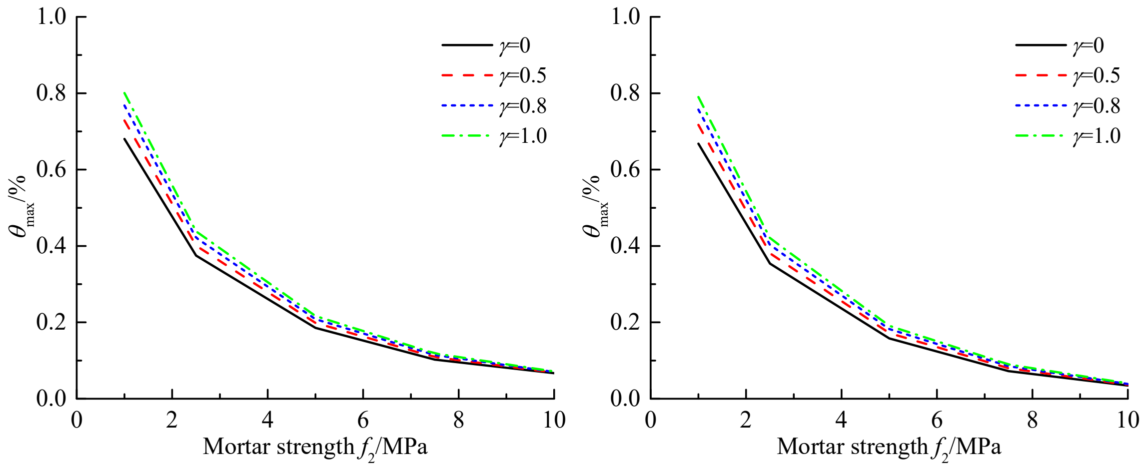

(c) (d)

Figure 11. The θ_{max} of masonry structures for different mortar strengths, PGA_{ms}=0.2g: (a) site class I, (b) site class II, (c) site class III, (d) site class IV.

For PGA_{ms} = 0.2g, the $\theta_{max,\gamma=1.0}/\theta_{max,\gamma=0}$ of the masonry structure with f_2= 1.0MPa, 2.5 MPa, 5.0 MPa, 7.5 MPa, and 10.0 MPa are 1.18, 1.18, 1.19, 1.11, and 1.04, respectively. For PGA_{ms} = 0.1g, the $\theta_{max,\gamma=1.0}/\theta_{max,\gamma=0}$ of the masonry structure with f_2= 1.0MPa, 2.5 MPa, 5.0 MPa, 7.5 MPa, and 10.0 MPa are 1.12, 1.06, 1.05, 1.04, and 1.04, respectively. The results show that the θ_{max} of masonry structures increase by 4.0% to 19.0%, which is consistent with the results of Section 4.2. The masonry structure with f_2= 1.0MPa has entered the inelastic phase when PGA_{ms} = 0.1g, and the masonry structure with f_2= 10.0MPa behaves elastically when PGA_{ms} = 0.2g, indicating that the masonry structure tends to remain elastic for higher seismic loads with the increase of mortar strength.

5. Summary and conclusions

The seismic response of masonry structures subjected to M-A sequences was investigated involving various parameters such as the aftershock intensity, the anti-seismic wall area ratio, the site classes, the number of storeys, and the mortar strength by using a simplified method newly proposed. The main conclusions are summarized as follows:

(1) On the basis of the non-iterative equivalent linearization method and the soft-storey failure mechanism of multi-storey masonry structures, an analytical method for the maximum storey drift (θ_{max}) of masonry structures subjected to M-A sequences was proposed. There was excellent agreement between analytical and numerical results for the θ_{max} of masonry structures

subjected to M-A sequences. The method proposed in this manuscript avoids iterative calculation and as a result, has a small workload and is easy to implement.

(2) The θ_{max} of masonry structures increases with the increase of aftershock intensity. The effect of aftershocks on masonry structures in plastic phase is more distinct than that in elastic phase. Furthermore, the effect of aftershock on the θ_{max} of masonry structures can be ignored when the relative intensity of the aftershock is less than 0.5, and the θ_{max} of masonry structures can increase by approximately 19.0% when the relative intensity of the aftershock equals 1.0.

(3) There is a significant variance for the θ_{max} of masonry structures subjected to M-A sequences on different site classes. The regardless of site class will lead to overestimation on the θ_{max} for site class I by 19.2% and underestimation on the θ_{max} for site class III by 17.6%.

(4) With the increase of anti-seismic wall area ratio (indicating the ratio of the total anti-seismic wall area at the 1/2-storey height to the storey area of the structure), the θ_{max} of masonry structures subjected to M-A sequences decreases drastically. By decreasing the anti-seismic wall ratio from 0.049 to 0.035, the θ_{max} increases to 2.60 times on average.

(5) With increasing number of storeys, the θ_{max} of masonry structures subjected to M-A sequences increases drastically. As the number of storeys decreases, the anti-overturning requirements and the base shear force of the masonry structures decrease, resulting in smaller θ_{max} and less damage.

(6) The effect of mortar strength on the θ_{max} of masonry structures subjected to M-A sequences is significant. Overall, the θ_{max} of the masonry structures with mortar strength equal to 2.5 MPa, 5.0 MPa, 7.5 MPa and 10.0 MPa is 0.55, 0.25, 0.11, and 0.05 times of that with mortar strength equal to 1.0 MPa, respectively.

Acknowledgements This work was financially supported by the National Key Research and Development Program of China (Grant No. 2017YFC0702900), Shanghai Rising-Star Program (Grant No. 20QB1404700) and Natural Science Foundation of Shanghai (Grant No. 21ZR1455000). Helpful suggestions provided by Dr. Shuo Yang are highly appreciated.

References

Apil K C, Sharma K, Pokharel B (2019) Performance of Heritage Structures during the Nepal Earthquake of April 25, 2015. Journal of Earthquake Engineering 23(8):1346-84.

Ates S, Kahya V, Yurdakul M, Adanur S (2013) Damages on reinforced concrete buildings due to consecutive earthquakes in Van. Soil Dynamics & Earthquake Engineering 53(10):109-18.

Azizi-Bondarabadi H, Mendes N, Loureno P B (2019) Higher Mode Effects in Pushover Analysis of Irregular Masonry Buildings. Journal of Earthquake Engineering 25(8):1459-93.

Borzi B, Calvi G M, Elnashai A S, Faccioli E, Bommer J J (2001) Inelastic spectra for displacement-based seismic design. Soil Dynamics & Earthquake Engineering 21(1): 47-61.

Borzi B, Crowley H, Pinho R (2008) Simplified pushover-based earthquake loss assessment (SP-BELTA) method for masonry buildings. International Journal of Architectural Heritage 2(4): 353-76.

CECS 160: 2004 (2004) General rule for performance-based seismic design of buildings (China Association for Engineering Construction Standardization). Planning Press, Beijing, China. [in Chinese]

EC8 (2004) Eurocode 8: design of structures for earthquake resistance - Part 1: General rules, seismic actions and rules for buildings, EN 1998-1, Draft 6, Doc CEN/TC250/SC8/N335, European Committee for Standardization (CEN), Brussels, Belgium.

Fajfar P (1999) Capacity spectrum method based on inelastic demand spectra. Earthquake Engineering & Structural Dynamics 28(9): 979-93.

GB50011–2010 (2010) Code for seismic design of buildings (National Standards of the People's Republic of China). Ministry of Construction of the People's Republic of China. [in Chinese]

Gledhill K, Ristau J, Reyners M, Fry B, Holden C (2011) The Darfield (Canterbury, New Zealand) Mw7.1 earthquake of September 2010: a preliminary seismological report. Seismological Research Letters 82(3): 378-86.

Goda K, Salami M R (2014) Inelastic seismic demand estimation of wood-frame houses subjected to mainshock-aftershock sequences. Bulletin of Earthquake Engineering 12(2): 855-74.

Graziotti F, Tomassetti U, Kallioras S, Penna A, Magenes G (2017) Shaking table test on a full scale URM cavity wall building. Bulletin of Earthquake Engineering 15: 5329-64.

Guerrini G, Graziotti F, Penna A, Magenes G (2017) Improved evaluation of inelastic displacement demands for short-period masonry structures. Earthquake Engineering & Structural Dynamics 46(9): 1411-30.

Hatzigeorgiou G D, Liolios A A (2010) Nonlinear behaviour of RC frames under repeated strong ground motions. Soil Dynamics & Earthquake Engineering 30(10): 1010-25.

Jiang L, Li X, Jiang L, Zhang F, Zheng S (2021) Shaking table tests on existing multi-story residence with installing elevators and seismic strengthening integrated technology. Journal of Building Structures 42(7): 20-9. [in Chinese]

Jiang L, Wang Z, Jiang L (2018) Approximate calculation method for fundamental period of multi-story masonry structures. Journal of Building Structures 39(S2): 254-262. [in Chinese]

Li X, Wen W, Zhai C (2020) A probabilistic framework for the economic loss estimation of structures considering multiple aftershocks. Soil Dynamics & Earthquake Engineering 133: 106121.

Li Q, Ellingwood B R (2010) Performance evaluation and damage assessment of steel frame buildings under main shock–aftershock earthquake sequences. Earthquake Engineering & Structural Dynamics 36(3): 405-27.

Lin Y, Lin Y (2009) Non-iterative equivalent linearization based on secant period for estimating maximum deformations of existing structures. Journal of Earthquake Engineering 13(2): 170-92.

Magenes G, Calvi G M (1997) In-plane seismic response of brick masonry walls. Earthquake Engineering & Structural Dynamics 26(11): 1091-112.

Mendes N, Loureno P B (2014) Sensitivity analysis of the seismic performance of existing masonry buildings. Engineering Structures 80: 137-46.

Nakamura Y, Derakhshan H, Griffith M C, Magenes G, Sheikh A H (2017) Applicability of nonlinear static procedures for low-rise unreinforced masonry buildings with flexible diaphragms. Engineering Structures 137: 1-18.

Newmark N M, Hall W J (1973) Seismic design criteria for nuclear reactor facilities. Report No 46, building practices for disaster mitigation. National Bureau of Standards, U.S. Department of Commerce: 209-36.

Priestley M J N, Calvi G M, Kowalsky M J (2007) Displacement-based seismic design of structures. Pavia: IUSS Press.

Raghunandan M, Liel A B, Luco N (2015) Aftershock collapse vulnerability assessment of reinforced concrete frame structures. Earthquake Engineering & Structural Dynamics 44:419-39.

Rinaldin G, Amadio C (2018) Effects of seismic sequences on masonry structures. Engineering Structures 166: 227-39.

Restrepo-Velez L F (2003) A simplified mechanics-based procedure for the seismic risk assessment of unreinforced masonry buildings. Individual Study. ROSE School, Pavia, Italy.

Shen J, Chen J, Ding G (2020) Random field model of sequential ground motions. Bulletin of Earthquake Engineering 18(11): 5119-41.

Shen J, Ren X, Zhang Y, Chen J (2019) Nonlinear dynamic analysis of frame-core tube building under seismic sequential ground motions by a supercomputer. Soil Dynamics & Earthquake Engineering 124(9): 86-97.

Tesfamariam S, Goda K (2015) Loss estimation for non-ductile reinforced concrete building in Victoria, British Columbia, Canada: effects of megathrust Mw 9-class subduction earthquakes and aftershocks. Earthquake Engineering & Structural Dynamics 44(13): 2303.

Tomaževič M (2007) Damage as a measure for earthquake resistant design of masonry structures: Slovenian experience. Canadian Journal of Civil Engineering 34(11): 1403-12.

Tomaževič M, Weiss P (2010) Displacement capacity of masonry buildings as a basis for the assessment of behavior factor: an experimental study. Bulletin of Earthquake Engineering 8(6): 1267-1294.

Tomić I, Vanin F, Beyer K (2021) Uncertainties in the Seismic Assessment of Historical Masonry Buildings. Applied Sciences 11(5): 2280.

USGS (2010) Aftershocks rattle Chile after earthquake, available online at: http://earthquake.usgs.gov/earthquakes/recenteqsww/Maps/10/290_-35.php.

Wang X, Wen W, Zhai C (2020) Vulnerability assessment of a high-rise building subjected to mainshock-aftershock sequences. Structural Design of Tall and Special Buildings: e1786.

Wang Z (2008) A preliminary report on the Great Wenchuan Earthquake. Earthquake Engineering & Engineering Vibration 7(2): 225-234.

Yeo G L, Cornell C A (2009) Building life-cycle cost analysis due to mainshock and aftershock occurrences. Structural Safety 31(5): 396-408.

Zhai C, Wen W, Li S, Xie L (2015) The ductility-based strength reduction factor for the mainshock-aftershock sequence-type ground motions. Bulletin of Earthquake Engineering 13(10): 2893-914.

Zhang Y (2020) Ductility-based strength reduction factor for mainshock-aftershock sequence-type ground motions. Building Structure 50(14): 97-103. [in Chinese]

Zhang Y, Chen J, Sun C (2017) Damage-based strength reduction factor for nonlinear structures subjected to sequence-type ground motions. Soil Dynamics & Earthquake Engineering 92(1):298-311.

Zhang Y, Lin X, Wang T, Skalomenos K (2021) Seismic behavior of masonry walls strengthened by precast reinforced concrete panels with different connection details. Engineering Structures 242(3): 112597.

Zhang Y, Shen J, Chen J (2020) Damage-based yield point spectra for sequence-type ground motions. Bulletin of Earthquake Engineering 18(10): 4705-24.

Zhang Y, Wang T (2013) Numerical simulation of masonry walls retrofitted by prefabricated reinforced concrete panels. 3rd International Conference on Civil Engineering, Architecture and Building Materials (CEABM 2013), 24-26 May, 2013, Jinan, China.

Zheng Q, Jiang L (2014) Calculation method for vertical load effect of masonry considering the cooperation of longitudinal and horizontal walls for existing buildings. Building science 31(SI): 379-85. [in Chinese]

Zhou B (2011) Experiences and future of earthquake-resisting of the masonry structure in China. Building Structure 41(9): 151-8. [in Chinese]